**Far East Journal of Mathematical Sciences (FJMS)**
Volume 53, Number 1, 2011, Pages 17-33
This paper is available online at http://pphmj.com/journals/fjms.htm


# MODELING AND OPTIMIZATION OF G-PROTEIN COUPLED RECEPTOR SIGNAL TRANSDUCTION

**CHARIN MODCHANG[1,3], BUSAYAMAS PIMPUNCHAT[1,6], WANNAPONG TRIAMPO[1,2,3], DARAPOND TRIAMPO[4] and YONGWIMON LENBURY[5]**

[1]R&D Group of Biological and Environmental Physics
Department of Physics
Faculty of Science
Mahidol University
Bangkok 10400, Thailand

[2]Institute for Innovative Learning
Faculty of Science
Mahidol University
Nakhon Pathom, Thailand

[3]ThEP Center, CHE, 328 Si Ayutthaya Road
Bangkok 10400, Thailand
e-mail: sccharin@mahidol.ac.th
wtriampo@gmail.com

[4]Department of Chemistry
Center of Excellence for Innovation in Chemistry
Faculty of Science
Mahidol University
Thailand
e-mail: scdar@mahidol.ac.th

2010 Mathematics Subject Classification: 93A30.

Keywords and phrases: G-protein coupled receptors, genetic algorithm, optimization, mathematical modeling, mathematical analysis.

Received February 4, 2011

[5]Department of Mathematics
Faculty of Science
Mahidol University
Bangkok 10400, Thailand
e-mail: scylb@mahidol.ac.th

*and*

Center of Excellence in Mathematics
PERDO, Commission on Higher Education
Thailand

[6]Department of Mathematics
Faculty of Science
Institute of Technology Ladkrabang
Bangkok 10520, Thailand
e-mail: knbusaya@kmitl.ac.th

**Abstract**

Signal transduction is the process by which a cell converts one kind of signal or stimulus into another. In this process, G-protein coupled receptors (GPCRs) are considered a major class of membrane protein receptors. GPCRs play a critical role in signal transduction, and they are important pharmacological drug targets. Motivated by some specific experimental data, we construct a mathematical model to investigate a signaling system of interest. The model is composed of mass-action ordinary differential equations that describe ligand-receptor and receptor-G-protein interactions. Because the kinetic reaction rates in the signaling processes previously gathered in reliable in vivo and in vitro experiments are limited to a small number of known values, we apply a genetic algorithm (GA) to estimate the parameter values in our model. In order to carry out the parameter estimation, we use the Augmented Lagrangian Genetic Algorithm (ALGA) with help from the mathematical theorem of infinite norm. This method ensures a faster parameter estimation speed in the modeled system. In addition, mathematical analyses are also performed. Some good agreement between analytic, numerical and experimental data was found. The simulation results of the model are extensively discussed and compared with the experimental data.

## 1. Introduction

Signal transduction is the process of converting external signals to a specific internal cellular response whose mechanisms consist of signaling elements which are organized in multi-protein complexes (such as hormones, growth factors and neurotransmitters) through protein-protein interactions [1-5]. In other words, signaling pathways span from the molecular level to their phenotypic and pathological effects. How the mechanism of signal transduction works is perhaps the most critical question surrounding our understanding of each physiological process. To uncover this mechanism, we use mathematical modeling in our work as a supplementary method to the experimental approach.

Typically, signal transduction consists of three processes: reception, transduction and response. It has been shown that G-protein coupled receptors (GPCRs) play an important role in transmembrane signal transduction. GPCRs represent the largest receptor family and are involved in the control of every aspect in pathological processes [6-8]. These receptors recognize extracellular signals to intracellular trimeric GTP-binding proteins, known as “G-proteins” (guanine nucleotide binding proteins), which in turn alter the activity of the enzymes or proteins involved in second messenger generation. How GPCRs operate is a fundamental question in the field of transmembrane signal transduction. To briefly demonstrate GPCR-based signal transduction, Figure 1 shows the mechanism of G-protein activation. The inactive form of the G-protein is heterotrimers composed of three subunits: $\alpha$, $\beta$ and $\gamma$ [9, 10]. A molecule of guanosine diphosphate (GDP) is bound to the $\alpha$ subunit. Binding of an agonist to a GPCR induces distinct conformational changes in the receptor protein that enables GPCR to promote a GDP release from the $\alpha$ subunit and a binding of the nucleotide guanosine triphosphate (GTP) at the same site. The G-protein is then released from the receptor and dissociates into separate $\beta\gamma$ and $\alpha$-GTP subunits. The $\alpha$-GTP is the active form of the G-protein. The activated $\beta\gamma$ and $\alpha$-GTP subunits then stimulate the generation of second messengers via intracellular effectors, passing on the signal by altering the activities of selected cellular proteins. In this work, we used a mathematical approach to understand specific experimental results of GPCR-based signal transduction.

Mathematical modeling is a powerful tool for analyzing complex biological systems [11, 12]. Recently, Modchang et al. [13] and Leelawattanachai et al. [14] proposed mathematical models for complex signal transduction models to explain

the dynamic trafficking and promiscuous coupling of G-protein coupled receptors. Their models are able to successfully explain the results observed in the laboratory. Since the biological systems that the authors wanted to explain are complex biological systems, it is obvious that they used complex mathematical models. Motivated by the experimental work of Yangthara et al. [15], we adopted a similar modeling approach in order to understand better their results. Due to the less complicated nature of *in vitro* results that are based on a simple biological system (e.g., there is no dynamic trafficking and promiscuous coupling of G-protein coupled receptors), we are faced with the question of whether a simple mathematical model can be used to explain the system instead of a complex mathematical model, and how accurate will be the results? To make our model more realistic, a genetic algorithm-based optimization is applied.

A genetic algorithm (GA) is an effective stochastic global search algorithm that is inspired by the evolutionary features of biological systems [16]. It has been successfully applied to various problems, such as function optimizations and parameter estimation in biochemical pathways [13, 14, 17-19]. The kinetic reaction rates of the signaling processes in reliable *in vivo* and *in vitro* experiments are currently limited to a small number of known values. Therefore, in the same manner as in [13], we have applied a GA to estimate the parameter values in our model. With the parameter values obtained by using the GA, the predictions of the model are then compared with the experimental results in [15].

## 2. Model Construction

For the purpose of testing our model, we have qualitatively reproduced the experimental results given in Figure 3 by Yangthara et al. [15]. Briefly, their experiment was performed on the vasopressin-2 receptor (V2R) as GPCR to produce data that reflect findings for a single well experiment. They measured the percentage of maximal activity from initial fluorescence slopes after $I^-$ addition as a function of forskolin and dDAVP concentrations in FRT-V2R and FRT-V2R-W164S cells. This percentage is considered a percentage of cellular response to an agonist, relative to the maximal response triggered by the same agonist. Since the experimental part is beyond the scope of this paper, we refer to [15] for more experimental details.

Based on the aforementioned experiment, we constructed a simple model to explain the dynamics of G-protein activation. Having realized the fact that the timing

and amplitude of signaling in cellular signaling pathways depend on the local concentrations and kinetics of component proteins, we formulated the deterministic model as follows. On the cell membrane, there are inactive or resting receptors, *R*; the numbers of ligand-bound receptors are denoted by $R_A$, while the activated ligand-bound receptor numbers are denoted by $R_A^*$. An activated ligand-bound receptor will bind to a G-protein, *G*, as shown in Figure 2. The parameters $k_a^+$ and $k_a^-$ represent rates of ligand association with, and dissociation from, an inactive receptor *R*, respectively. The ligand-bound receptors $R_A$ are reversibly converted to an active state $R_A^*$ with rate constants $L^+$ and $L^-$, respectively. Ligand-bound activated receptors $R_A^*$, associate with and dissociate from the G-protein, denoted by *G*, with rate constants $k_g^+$ and $k_g^-$. The inactive form of the G-protein consists of α, β and γ subunits, with a molecule of GDP bound to the α subunit $(G_\alpha)$. The interaction of this inactive G-protein with a ligand-bound activated receptor promotes the release of GDP from the α subunit and the binding of GTP at the same site. We have assumed that the dissociation of GDP and association of GTP happen instantaneously, and that the activated receptor activates the G-protein at the rate constant $k_{act}$. Active G-proteins are returned to their inactive state upon hydrolysis of GTP by the GTPase activity. In our model, we assume that the inactivation of the G-protein is so fast for this time scale that it is described as a one-step process with a rate constant $k_d$.

From the model structure in Figure 2, and based on the principles of mass action kinetics, the system of equations can be derived as:

$$\frac{dR}{dt} = -k_a^+ AR + k_a^- R_A, \tag{1}$$

$$\frac{dR_A^*}{dt} = L^+ R_A - L^- R_A^* - k_g^+ G R_A^* + k_g^- R_{AG}^* + k_{act} R_{AG}^*, \tag{2}$$

$$\frac{dR_{AG}^*}{dt} = k_g^+ G R_A^* - k_g^- R_{AG}^* - k_{act} R_{AG}^*, \tag{3}$$

$$\frac{dG^*}{dt} = k_{act} R_{AG}^* - k_d G^*, \tag{4}$$

$$R_A = R_0 - R - R_A^* - R_{AG}^*, \tag{5}$$

$$G = G_0 - G^* - R_{AG}^*. \tag{6}$$

In order to obtain the model equations, we assume that the total number of receptors and G proteins on the cell membrane and the concentration of ligands, denoted by $A$, remain constant.

## 3. Nondimensionalization

We now proceed to carry out nondimensionalization by the following rescaling:

$$R = R_0\tilde{R}, \quad G = G_0\tilde{G}, \quad t = \tilde{t}\,/k_a^-, \quad A = a_0\tilde{A},$$

$$\tilde{k}_a^+ = \frac{k_a^+}{k_a^-}a_0, \quad \tilde{L}^+ = \frac{L^+}{k_a^-}, \quad \tilde{L}^- = \frac{L^-}{k_a^-}, \quad \tilde{k}_g^+ = \frac{k_g^+}{k_a^-}G_0,$$

$$\tilde{k}_g^- = \frac{k_g^-}{k_a^-}, \quad \tilde{k}_{act} = \frac{k_{act}}{k_a^-}, \quad \tilde{k}_d = \frac{k_d}{k_a^-}.$$

Substitute this scaling into equations (1)-(6). Overbars will be dropped henceforth for brevity. The nondimensionalized system of equations is then:

$$\frac{dR}{dt} = -k_a^+AR + R_A, \tag{7}$$

$$\frac{dR_A^*}{dt} = L^+R_A - L^-R_A^* - k_g^+GR_A^* + k_g^-R_{AG}^* + k_{act}R_{AG}^*, \tag{8}$$

$$\frac{dR_{AG}^*}{dt} = k_g^+GR_A^* - k_g^-R_{AG}^* - k_{act}R_{AG}^*, \tag{9}$$

$$\frac{dG^*}{dt} = k_{act}NR_{AG}^* - k_dG^*, \tag{10}$$

$$R_A = 1 - R - R_A^* - R_{AG}^*, \tag{11}$$

$$G = 1 - G^* - NR_{AG}^*, \tag{12}$$

where $N \equiv R_0/G_0$. Substituting equations (11)-(12) into equations (7)-(10) leads to:

$$\frac{dR}{dt} = 1 - (k_a^+ A + 1)R - R_A^* - R_{AG}^*, \tag{13}$$

$$\frac{dR_A^*}{dt} = L^+ - L^+ R - (L^- + L^+ + k_g^+)R_A^* + (k_g^- + k_{act} - L^+)R_{AG}^* + k_g^+ G^* R_A^* + k_g^* N R_{AG}^* R_A^*, \tag{14}$$

$$\frac{dR_{AG}^*}{dt} = k_g^+ R_A^* - (k_g^- + k_{act})R_{AG}^* - k_g^+ G^* R_A^* - k_g^+ N R_{AG}^* R_A^*, \tag{15}$$

$$\frac{dG^*}{dt} = k_{act} N R_{AG}^* - k_d G^*. \tag{16}$$

Since the binding of the G-protein to an activated receptor often leads to the activation of the G-protein, we assume that the G-protein activation-rate constant $k_{act}$ is very large and the G-protein dissociation-rate constant $k_g^-$ is very small. Now, let us make some approximations by letting

$$\varepsilon = \frac{k_a^-}{k_{act}} = \frac{1}{\tilde{k}_{act}}, \text{ where } \varepsilon << 1.$$

It is reasonable to rescale $R_{AG}^*$ by letting $R_{AG}^* = \varepsilon \tilde{R}_{AG}^*$; then our system of equations becomes:

$$\frac{dR}{dt} = 1 - (k_a^+ A + 1)R - R_A^* - \varepsilon R_{AG}^*, \tag{17}$$

$$\frac{dR_A^*}{dt} = L^+ - L^+ R - (L^- + L^+ + k_g^+)R_A^* + \left(k_g^- + \frac{1}{\varepsilon} - L^+\right)\varepsilon R_{AG}^* + k_g^+ G^* R_A^* + \varepsilon k_g^* N R_{AG}^* R_A^*, \tag{18}$$

$$\frac{dR_{AG}^*}{dt} = \frac{1}{\varepsilon} k_g^+ R_A^* - \left(k_g^- + \frac{1}{\varepsilon}\right)R_{AG}^* - \frac{1}{\varepsilon} k_g^+ G^* R_A^* - k_g^+ N R_{AG}^* R_A^*, \tag{19}$$

$$\frac{dG^*}{dt} = N R_{AG}^* - k_d G^*. \tag{20}$$

By assuming that $\varepsilon << 1$, we obtain the following system of equations:

$$\frac{dR}{dt} = 1 - (k_a^* A + 1)R - R_A^*, \tag{21}$$

$$\frac{dR_A^*}{dt} = L^+ - L^+ R - (L^- + L^+)R_A^*, \tag{22}$$

$$R_{AG}^* = k_g^+ R_A^* (1 - G^*), \tag{23}$$

$$\frac{dG^*}{dt} = R_{AG}^* - k_d G^*. \tag{24}$$

Substitute (23) into (24), we have

$$\frac{dG^*}{dt} = k_g^+ R_A^* - (k_g^+ R_A^* + k_d)G^*. \tag{25}$$

## 4. Parameters Estimations

To do the parameter estimations, we start from equations (17)-(20). Using the limit $\varepsilon \to 0$, with a quasi-steady state approximation for $G^*$, we solve equations (19) and (20) for $R_{AG}^*$ and $G^*$ and then substitute this into equations (17) and (18),

$$\frac{dR}{dt} = 1 - (k_a^+ A + 1)R - R_A^*, \tag{26}$$

$$\frac{dR_A^*}{dt} = L^+ - L^+ R - (L^- + L^+)R_A^*, \tag{27}$$

$$R_{AG}^* = k_g^+ R_A^* (1 - G^*), \tag{28}$$

$$G^* = \frac{H}{1 + H}, \tag{29}$$

where $H = \frac{Nk_g^+ R_A^*}{k_d}$. Next, we transform our model equations to a system of finite difference equations, $\vec{u}^{k+1} = \mathbf{A}\vec{u}^k + \vec{b}$, by using the forward time scheme,

$$\frac{R^{(i+1)} - R^{(i)}}{\Delta t} = 1 - (k_a^+ A + 1) R^{(i)} - R_A^{*(i)},$$

$$\frac{R_A^{*(i+1)} - R_A^{*(i)}}{\Delta t} = L^+ - L^+ R^{(i)} - (L^- + L^+) R_A^{*(i)}.$$

This can be rearranged and written it in the matrix form:

$$\begin{bmatrix} R^{(i+1)} \\ R_A^{*(i+1)} \end{bmatrix} = \begin{bmatrix} 1 - \Delta t(k_a^+ A + 1) & -\Delta t \\ -\Delta t L^+ & 1 - \Delta t(L^- + L^+) \end{bmatrix} \begin{bmatrix} R^{(i+1)} \\ R_A^{*(i+1)} \end{bmatrix} + \begin{bmatrix} \Delta t \\ \Delta t L^+ \end{bmatrix}. \quad (30)$$

Our model equations (26)-(29) contain 5 unknown parameters ($k_a^+$, $L^+$, $L^-$, $k_g^+$ and $k_d$), but the experimental data available from the literatures are limited to only a few parameters [20]. So, next we use a genetic algorithm (GA) to estimate these unknown parameters.

A genetic algorithm is an effective stochastic global search algorithm that mimics biological evolution [16]. It is an optimization technique that was developed by Holland and his colleagues in 1975. GA produces optimum solutions by mimicking two biological mechanisms: natural selection and sexual reproduction. Both natural selection and sexual reproduction allow organisms to evolve while generations pass. In our problem, the input to the GA is a set of vectors whose elements are the values of those 5 parameters. A fitness function is defined to be the distance $f(\mathbf{x})$ measured between experimental and predicted values of the steady state activated G-protein concentration,

$$f(\mathbf{x}) = \left( \sum_{i=1}^{n} | y_{\text{pred}}(i) - y_{\text{exp}}(i) | \right)^2, \quad (31)$$

where $n$ is the number of data points for each experiment; $y_{\text{exp}}$ represents the known experimental data; and $y_{\text{pred}}$ is the predicted results of the steady state activated G-protein concentration obtained by using the GA. The purpose of the GA is to produce successive populations of individuals, which are generated with the aim of decreasing the distance $f(\mathbf{x})$ between the simulated data and experimental data.

In order to estimate the parameter values, we make use of a mathematical theorem, Theorem 2.5.2 in [21], which states that:

*If an infinity norm of* **A**, $\| \mathbf{A} \|$, *is less than one, then the iteration scheme* $\vec{u}^{k+1} = \mathbf{A}\vec{u}^{k} + \vec{b}$ *converges to the steady state equation,*

$$\vec{u} = (\mathbf{I} - \mathbf{A})^{-1}\vec{b}, \tag{32}$$

*where* **I** *is the identity matrix and the infinity norm of matrix* **A** *is defined by*

$$\| \mathbf{A} \| \equiv \max_i \sum_j |a_{ij}|.$$

By using this theorem, the steady state solutions of our model equation (55) then become

$$\begin{bmatrix} R \\ R_A^* \end{bmatrix} = \begin{bmatrix} (k_a^+ A + 1) & 1 \\ L^+ & (L^- + L^+) \end{bmatrix}^{-1} \begin{bmatrix} 1 \\ L^+ \end{bmatrix}. \tag{33}$$

Thus, in generating a parameter estimation, we also impose a nonlinear constraint $\| \mathbf{A} \| < 1$. More details regarding how we performed the parameter estimation can be found in [13]. To save optimization time, in addition to the constraint that $\| \mathbf{A} \| < 1$, we also imposed lower and upper bounds between 0.001-2500 on each parameter. The GA was performed by using 25 individuals of population, and was run up to 100 generations.

## 5. Results and Discussion

Numerically, we rescaled the agonist concentrations by using $a_0 = 10^6 \mathrm{M}^{-1}$, and for the purpose of good parameter estimation, we interpolated the experimental data seen in Figure 3 in [15] by using their experimentally fitted curve from 7 points to 51 points. Via MATLAB® 7.8 on a personal computer with Intel® Core 2 Duo CPU and 2 GB of RAM, the GA was run 50 times. It took less than 5 minutes per run.

The best fitness value from 50 runs was about 4. Examples of the numerical solutions of the steady state activated G-protein concentration versus agonist concentrations of 4 independent runs are shown in Figure 3, after assuming that $N \equiv R_0 / N_0 = 1$. The obtained parameter values from 4 representative runs are

shown in Table 1. As can be seen, good agreement between the experimental and numerical data was found. Still, the stochastic variation associated with each numerical curve is mainly due to the searched parameters or optimal chromosome set. Because of this, the obvious question becomes what set of parameters should be selected. In our presentation, for example, there are four sets to be justified. In order to select the best parameter, some experimentally measured parameter values or sensible estimates are crucially required. However, measurement of these parameters is beyond the scope of this paper, thus we only bring it up as a subject to be addressed in future research.

Figure 4 represents the time evolution of the fitness value for four representative runs. Hence the mean fitness is an average of fitness of population in each generation. In this case, the GA is terminated when there is no change of mean fitness within 100 generations. In fact, the GA once again gives slightly different results for each run because of their stochastic characteristics. After performing several runs, it was found that the initial fitness values for various runs are very broad (in the 5-600 range), while the final fitness values are very narrow (in the 4-10 range). We can see that the numerical results from RUN1 and RUN2 are comparatively very close together, although their parameter values (see Table 1) are not the same. From the parameter values, it is seen that the ratios $L^+ : k_a^+$ in RUN3 and RUN4 are much greater than those of RUN1 and RUN2. This indicates that the parameters corresponding to RUN3 are less favorable on $R_A$. The ratios $L^- : L^+$ in RUN1, RUN2, RUN3 and RUN4 are 183.04, 121.7, 2.54 and 0.936, respectively. In an approximate sense, the $L^- : L^+$ ratio may be well correlated with the $R_A : R_A^*$ ratio. Since our solving approach does absorb parameter $k_a^-$, it is impossible to provide any information regarding $R$ and $R_A$. In our view, these receptors are parameters which could be feasible to measure experimentally.

These findings may suggest useful input information to experimentalists. It should be mentioned that, in chemical reaction kinetics, chemical binding is at least a two-step process that includes the transporting of reagents, receptors, and ligands, and biochemical reactions or binding interactions. Therefore, all rate constants being used here are a combination rate of both transport and reaction events. Note, however, that the system under investigation does not guarantee that the inverse problem has one unique solution. We can only say that the obtained solutions (e.g., the parameter values from RUN1-RUN4) are good solutions, because they give good

predictions of the activated G-protein concentrations that are close to the experimental data. However, their correctness must be confirmed by comparing them with the experimental values, since these predictions might not be the true solution. As can be seen in Figure 5, although these solutions give quite similar G-protein concentrations, they all predict quite different amounts of activated ligand bound receptors, $R_A^*$. So, if we experimentally know the amount of $R_A^*$ for different receptor or G-protein states, then this will provide important evidence to justify which parameter set may be the most suitable or practicable one.

By using the linear stability analysis, we also find the analytical solutions of our model. As a demonstration propose, we then use the parameters values from RUN1 to plot the analytical solutions of $R$, $R_A^*$ and $G^*$, Figure 6(a) shows the comparison between the analytical solutions and numerical solutions. The numerical solutions are found by numerically solving the model without any approximation. We can see that when these analytical and its corresponding numerical solutions are close to the steady state, the solutions converge to the same values. In fact, these $R$, $R_A^*$ and $G^*$ concentrations are close together before going to a steady state. By comparing the analytical and numerical solutions of $G^*$, it was found that $G^*$ corresponding to the quasi-steady state solution reasonably reaches steady state solution much more rapidly than those corresponding analytical and numerical solutions. It is evidently shown in Figure 6(b) which is plotted by using the parameters values in RUN1.

## 6. Conclusions

In this work, we proposed a simple mathematical model to explain the experimental results of interest. The lack of measurable kinetic interaction rates in reliable *in vivo* and *in vitro* experiments is currently the major limitation of signaling pathway models. Thus, we used a constrained genetic algorithm to estimate sets of unknown parameters. Although our proposed model is relatively simple compared to the models proposed by other works [13, 14], it was able to predict the dose-response curve observed by the authors in [15].

## Acknowledgments

The authors thank David Blyler for editing the manuscript and providing helpful comments. This research project is supported by Faculty of Science, Mahidol

University, the Thailand Research Fund (TRF), the Commission on Higher Education, Ministry of Education, Mahidol University Research Grant, Center of Excellence for Innovation in Chemistry (PERCH-CIC) and The Thailand Center of Excellence in Physics (ThEP).

## References

[1] A. Persidis, Signal transduction as a drug-discovery platform, Nat. Biotech. 16(11) (1998), 1082-1083.

[2] A. P. Somlyo and A. V. Somlyo, Signal transduction by G-proteins, rho-kinase and protein phosphatase to smooth muscle and non-muscle myosin II, The Journal of Physiology 522(2) (2000), 177-185.

[3] D. R. Flower, Modelling G-protein-coupled receptors for drug design, Biochimica et Biophysica Acta (BBA) - Reviews on Biomembranes 1422(3) (1999), 207-234.

[4] M. Marinissen and J. Gutkind, G-protein-coupled receptors and signaling networks: emerging paradigms, Trends in Pharmacological Sciences 22(7) (2001), 368-376.

[5] A. Levitzki and S. Klein, Signal transduction therapy of cancer, Molecular Aspects of Medicine, 31 (2010), 287-329.

[6] M. Simon, M. Strathmann and N. Gautam, Diversity of *G* proteins in signal transduction, Science 252(5007) (1991), 802.

[7] S. Hill, G-protein-coupled receptors: past, present and future, British Journal of Pharmacology 147(S1) (2006), S27-S37.

[8] G. Milligan, A day in the life of a G protein-coupled receptor: the contribution to function of *G* protein-coupled receptor dimerization, British Journal of Pharmacology 153(S1) (2008), S216-S229.

[9] D. A. Lauffenburger and J. J. Linderman, Receptors: Models for Binding, Trafficking, and Signaling, Oxford University Press, USA, 1993.

[10] S. R. Neves, P. T. Ram and R. Iyengar, G protein pathways, Science 296(5573) (2002), 1636-1639.

[11] A. Alam-Nazki and J. Krishnan, A mathematical modelling framework for understanding chemorepulsive signal transduction in Dictyostelium, J. Theor. Biol. 266(1) (2010), 140-153.

[12] W. S. Hlavacek et al., Rules for modeling signal-transduction systems, Sci. STKE 2006(344) (2006), re6.

[13] C. Modchang, W. Triampo and Y. Lenbury, Mathematical modeling and application of genetic algorithm to parameter estimation in signal transduction: Trafficking and promiscuous coupling of G-protein coupled receptors, Computers in Biology and Medicine 38(5) (2008), 574-582.

[14] J. Leelawattanachai et al., Modeling and genetic algorithm optimization of early events in signal transduction via dynamics of G-protein-coupled receptors: Internalization consideration, Appl. Math. Comput. 207(2) (2009), 528-544.

[15] B. Yangthara et al., Small-molecule vasopressin-2 receptor antagonist identified by a G-protein coupled receptor "pathway" screen, Mol. Pharmacol. 72(1) (2007), 86-94.

[16] J. H. Holland, Adaptation in Natural and Artificial Systems, MIT Press, Cambridge, MA, USA, 1992.

[17] L. J. Park et al., Application of genetic algorithms to parameter estimation of bioprocesses, Med. Biol. Eng. Comput. 35(1) (1997), 47-49.

[18] C. G. Moles, P. Mendes and J. R. Banga, Parameter estimation in biochemical pathways: a comparison of global optimization methods, Genome Res. 13(11) (2003), 2467-2474.

[19] I. Arisi, A. Cattaneo and V. Rosato, Parameter estimate of signal transduction pathways, BMC Neurosci. 7(Suppl 1) (2006), S6.

[20] C. Starbuck and D. A. Lauffenburger, Mathematical model for the effects of epidermal growth factor receptor trafficking dynamics on fibroblast proliferation responses, Biotechnol. Prog. 8(2) (1992), 132-143.

[21] R. E. White, Computational Mathematics: Models, Methods and Analysis with MATLAB and MPI, CRC Press, 2004.

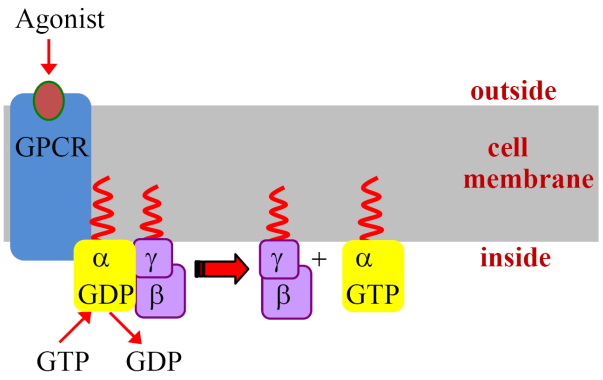


**Figure 1.** Schematic representation of G-protein activation.

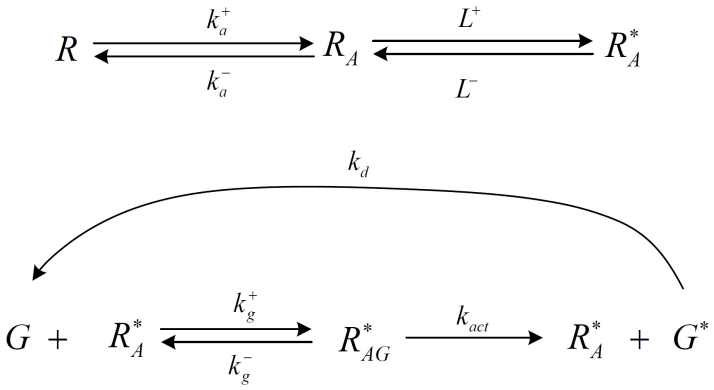


**Figure 2.** Model structure of receptor-ligand binding and G-protein activation.

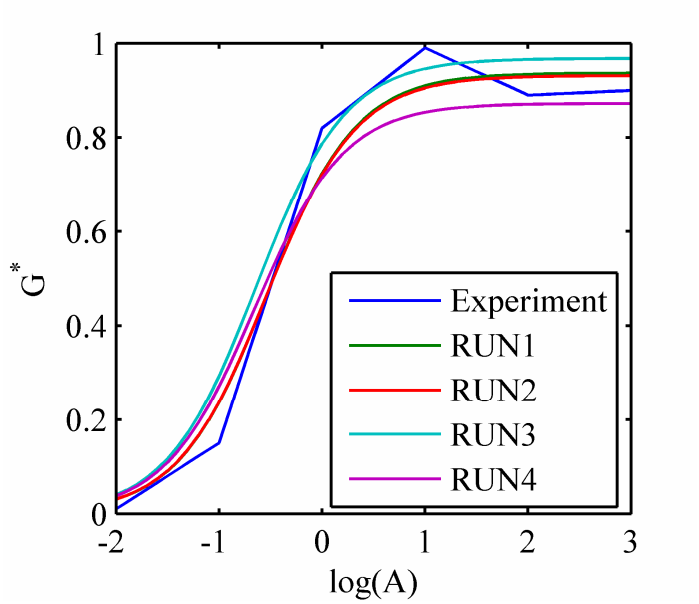


**Figure 3.** Comparison of the normalized activated G-protein concentrations at various agonist concentrations. The numerical results (RUN1-RUN4) were obtained by using the parameter values in RUN1, RUN2, RUN3, RUN4 and equations (28), (29) and (33). The blue line represents the experimental results from [15].

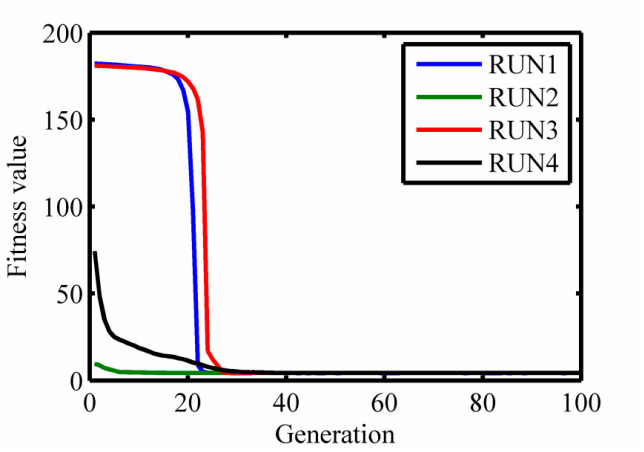


**Figure 4.** Time evolution of the fitness value for three representative runs.

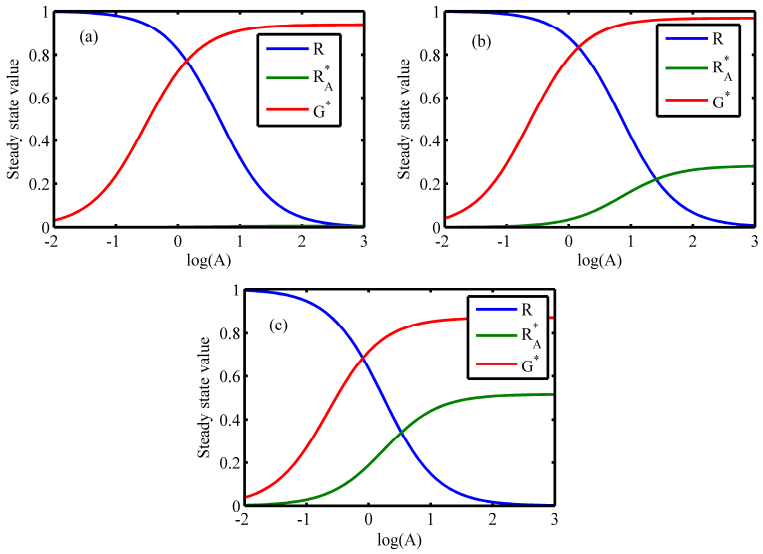


**Figure 5.** Steady state values of $R$, $R_A^*$ and $G^*$ as a function of agonist concentration (in log scale). These steady state values were obtained by using parameter values from RUN1 (a), RUN3 (b) and RUN4 (c). It can be seen that although the parameter values from RUN1, RUN2 and RUN3 give a similar prediction of $G^*$, they all give a different prediction of $R_A^*$. Note that the result for the parameter values in RUN2 is very similar to that for RUN1 and is not shown here.

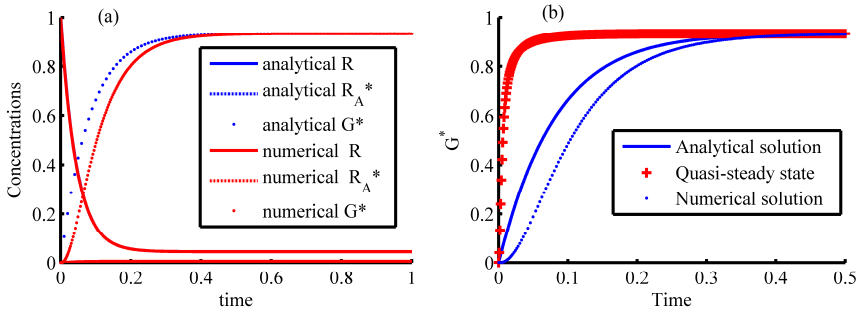


**Figure 6.** (a) Comparison between analytical and numerical solutions of $R$, $R_A^*$ and $G^*$, (b) Comparison of the G-protein concentrations.

**Table 1.** The parameter values for concentrations and response curves obtained by using genetic algorithm. Four independent runs were performed to obtain the 4 sets of parameter values

| Parameter | Values | | | |
|---|---|---|---|---|
| | RUN1 | RUN2 | RUN3 | RUN4 |
| $k_a^+$ | 0.212 | 0.233 | 0.100 | 0.278 |
| $L^+$ | 1.630 | 4.050 | 983.314 | 2068.838 |
| $L^-$ | 298.352 | 492.890 | 2500 | 1937.134 |
| $k_g^+$ | 2336.088 | 1969.798 | 2500 | 929.988 |
| $k_d$ | 0.854 | 1.179 | 23.384 | 70.109 |
| Fitness value | 4.099 | 4.139 | 6.293 | 9.114 |